

# Time Optimal Attitude Control of Asymmetric Rigid Spacecraft

R. M. BYERS

*Department of Mechanical & Aerospace Engineering, University of Central Florida, Orlando, FL 32765, U.S.A.*

(Received 12 June 1995, accepted 5 September 1995)

**Abstract:** Time optimal *rest-to-rest* reorientation of a rigid spacecraft with an arbitrary initial attitude and distinct principal moments of inertia is discussed. The effect of the gyroscopic coupling terms in Euler's equations on the control switch times is shown. A method for recursively generating coefficients for a truncated Taylor series solution of Euler's equations and the differential equations for the Euler parameter state transition matrix is shown. These solutions are used to solve for the optimal control switch times.

**Key Words:** Time optimal control, rest-to-rest, bang-bang

## 1. INTRODUCTION

Minimum time attitude changes for a rigid spacecraft have been the subject of numerous studies in the recent literature. For the *rest-to-rest* maneuver, it is determined from the necessary conditions that the controls must be *bang-bang* and that no singular intervals exist. Notably, Bilimoria and Wie (1993) found that for a symmetric body, the time optimal reorientation state trajectory did not correspond to a rotation about a fixed axis. Subsequently, they examined the time optimal rotation of an axisymmetric body (1991). Seywald and Kumar (1993) examined the necessary conditions for singular controls in time optimal maneuvers of a symmetric body, but did not specifically determine whether singular arcs were possible in the rest-to-rest time optimal maneuver. Byers (1995) determined that singular controls could not satisfy the rest-to-rest boundary conditions for time optimal reorientation.

Byers and Vadali (1993) determined that for a symmetric body with three control axes, rest-to-rest reorientation can be achieved with bang-bang controls and five control switches separating six time intervals over which the control vector is constant. Furthermore, it was observed that the sequence and duration of the final three intervals are identical to the first three with the sign of the control vector reversed. From this observation, an approximate solution of the state transition matrix for the Euler parameters was developed, which allows real time estimation of the switch times. The accuracy of the solution is degraded for large angle rotations. In addition, for nonsymmetric spacecraft, the angular velocity differential equations are no longer linear. The sometimes significant gyroscopic coupling encountered has the effect of *skewing* the symmetry of the switch times.

In the present paper, time optimal rotation of a body with arbitrary moments of inertia is considered. The effect of gyroscopic coupling on the solution of the angular

velocity and Euler parameter vectors is examined. An accurate solution to the control switch times requires an improved solution to the angular velocity and Euler parameter vectors. A method for solving for the angular velocities and Eulerian angles of a symmetric spacecraft developed by Tsiotras and Longuski (1991) depends on small angle approximations. Morton, Junkins, and Blanton (1974) suggest a Taylor series solution for the angular velocity and Euler parameter vectors. In the present work, we adopt the Taylor series of Morton et al. (1974) to determine the state transition matrix between control switches. By assuming that the optimal control consists of five control switches, the time intervals between the switches can be determined for all possible switching sequences. The results are compared to the optimal switch times determined by solution of the Two-Point-Boundary-Value-Problem (TPBVP).

## 2. RIGID BODY DYNAMICS

The attitude state of a rigid body may be described by the  $7 \times 1$  vector

$$\underline{x}(t) = \begin{Bmatrix} \underline{\omega}(t) \\ \underline{\beta}(t) \end{Bmatrix}, \quad (1)$$

where  $\underline{\omega}(t)$  is the  $3 \times 1$  vector of body fixed components of angular velocity and  $\underline{\beta} = [\beta_1 \ \beta_2 \ \beta_3 \ \beta_0]^T$  is the  $4 \times 1$  vector of Euler parameters where

$$\begin{aligned} \beta_i &= l_i \sin\left(\frac{\theta}{2}\right) \quad i = 1, 2, 3 \\ \beta_0 &= \cos\left(\frac{\theta}{2}\right). \end{aligned} \quad (2)$$

$l_i$  are the components of a  $3 \times 1$  unit Euler axis about which a rotation of angle  $\theta$  will bring a body fixed frame into coincidence with an inertial frame.

The differential equations for angular velocity of a rigid body are given by Euler's equations

$$\dot{\underline{\omega}} = \mathbf{I}^{-1}(\tilde{\omega}\mathbf{I}\underline{\omega}) + \mathbf{I}^{-1}\mathbf{B}\underline{u}, \quad (3)$$

where  $\tilde{\omega}$  is the skew symmetric cross product matrix operator

$$\tilde{\omega} = \begin{bmatrix} 0 & \omega_3 & -\omega_2 \\ -\omega_3 & 0 & \omega_1 \\ \omega_2 & -\omega_1 & 0 \end{bmatrix}$$

and  $\underline{u}$  is the  $m \times 1$  control vector,  $\mathbf{I}$  is the  $3 \times 3$  inertia matrix, and  $\mathbf{B}$  is the constant  $3 \times m$  control influence matrix.

The three-axis normalized control vector is constrained such that

$$|u_i| \leq 1 \quad i = 1, 2, 3. \quad (4)$$

The present work is restricted to control torques of equal magnitude along the principle axes, that is,  $\mathbf{B} = BE_3$  where  $B$  is a saturation torque magnitude and  $E_3$  is the  $3 \times 3$  identity

matrix. Redefining the control vector  $\underline{v} = \mathbf{I}^{-1}\mathbf{B}\underline{u}$  allows the equations of motion to be written

$$\begin{aligned}\dot{\omega}_1 &= \alpha_1 \omega_2 \omega_3 + v_1 \\ \dot{\omega}_2 &= \alpha_2 \omega_1 \omega_3 + v_2 \\ \dot{\omega}_3 &= \alpha_3 \omega_1 \omega_2 + v_3,\end{aligned}\tag{5}$$

where

$$\begin{aligned}\alpha_1 &= \frac{I_2 - I_3}{I_1} \\ \alpha_2 &= \frac{I_3 - I_1}{I_2} \\ \alpha_3 &= \frac{I_1 - I_2}{I_3}.\end{aligned}$$

It is observed that the moments of inertia are constrained such that  $I_i < I_j + I_k$  where  $i, j, k$  are any nonrepeating permutation of 1, 2, 3. This gives the constraint

$$-1 < \alpha_i < 1 \quad i = 1, 2, 3.\tag{6}$$

For an axisymmetry body, one of the  $\alpha_i$  is zero; the other two are equal in magnitude and of opposite sign.

The differential equations for the Euler parameters are given by the matrix equation

$$\frac{d}{dt}\underline{\beta}(t) = \frac{1}{2}\mathbf{G}(\underline{\omega})\underline{\beta}(t),\tag{7}$$

where

$$\mathbf{G}(\underline{\omega}) = \begin{bmatrix} 0 & \omega_3 & -\omega_2 & \omega_1 \\ -\omega_3 & 0 & \omega_1 & \omega_2 \\ \omega_2 & -\omega_1 & 0 & \omega_3 \\ -\omega_1 & -\omega_2 & -\omega_3 & 0 \end{bmatrix}.$$

### 3. OPTIMAL CONTROL PROBLEM

The time optimal control minimizes the performance index

$$J = \int_{t_0}^{t_f} dt.\tag{8}$$

The Hamiltonian is

$$\mathcal{H} = 1 + \underline{\lambda}_\omega^T \underline{\dot{\omega}} + \underline{\lambda}_\beta^T \underline{\dot{\beta}},\tag{9}$$

where  $\underline{\lambda} = [\underline{\lambda}_\omega^T, \underline{\lambda}_\beta^T]^T$  is the  $7 \times 1$  costate vector. Because the final time is free and the Hamiltonian is not an explicit function of time,  $\mathcal{H} \equiv 0$ . The costate differential equations

are given by

$$\begin{aligned}\dot{\underline{\lambda}} &= -\frac{\partial \mathcal{H}}{\partial x} \\ \dot{\lambda}_\omega &= -\frac{1}{2}\mathbf{F}(\underline{\beta})\underline{\lambda}_\beta - \Omega\underline{\lambda}_\omega\end{aligned}\quad (10)$$

$$\dot{\lambda}_\beta = \frac{1}{2}\mathbf{G}(\omega)\underline{\lambda}_\beta, \quad (11)$$

where

$$\mathbf{F}(\underline{\beta}) = \begin{bmatrix} \beta_0 & \beta_3 & -\beta_2 & -\beta_1 \\ -\beta_3 & \beta_0 & \beta_1 & -\beta_2 \\ \beta_2 & -\beta_1 & \beta_0 & -\beta_3 \end{bmatrix}, \quad \Omega = \begin{bmatrix} 0 & \alpha_2\omega_3 & \alpha_3\omega_2 \\ \alpha_1\omega_3 & 0 & \alpha_3\omega_1 \\ \alpha_1\omega_2 & \alpha_2\omega_1 & 0 \end{bmatrix}.$$

Applying Pontryagin's Principle leads to the optimal control

$$u_i^* = -\text{sign}\left(\frac{\partial \mathcal{H}}{\partial u_i}\right) = -\text{sign}(\lambda_{\omega_i}) \quad i = 1, 2, 3. \quad (12)$$

The transversality condition gives the costates at the final time

$$\underline{\lambda}^T(t_f) = \underline{\nu}^T \left[ \frac{\partial \Psi}{\partial x(t_f)} \right] = [\underline{\nu}^T \quad 0], \quad (13)$$

where

$$\underline{\Psi} = [\omega_1(t_f) \quad \omega_2(t_f) \quad \omega_3(t_f) \quad \beta_1(t_f) \quad \beta_2(t_f) \quad \beta_3(t_f)]^T \quad (14)$$

and  $\underline{\nu}$  is a  $6 \times 1$  vector of constant multipliers.

The two-point boundary value problem may be solved by a number of numerical methods. From equation (12) it is seen that the control will be bang-bang except in the singular control case where one or more of the switching functions  $\lambda_{\omega_i} = 0$  for some finite time interval. The Switch Time Optimization (STO) algorithm developed by Meier and Bryson (1990) is a first-order gradient method for solving the time optimal switch times using bang-bang controls for a two-link manipulator. In this paper, the STO algorithm is modified to numerically solve for the switching functions and the optimal control for rigid body maneuvers.

#### 4. CHARACTERISTICS OF THE TIME OPTIMAL REST-TO-REST MANEUVER

Byers and Vadali (1993) demonstrated that multi-axis rotations of a symmetric rigid body with three-axis control require a minimum of five control switches with six control intervals  $\Delta_i$ ,  $i = 1, \dots, 6$  over which the control vector is constant. One of the control axes has a single control switch. This axis is designated the *critical axis*. The other two controls switch twice. The author, as well as Bilimoria and Wie (1993), found in numerical simulations that time optimal large angle rotations about a control axis are in fact characterized by five switches. For rotation angles less than  $73^\circ$ , Bilimoria and Wie found that the

optimal maneuver possesses seven switches. The author also shows that the difference between final times found for the seven-switch maneuver and the five-switch maneuver is approximately 0.23% for a rotation angle of  $45^\circ$  and decreases for smaller angles. In cases other than principal axis rotations, the author has observed only the five-switch solution, which, even when not exactly optimal, is very near optimal.

In general, Euler's equations may be considered to consist of two components

$$\dot{\underline{\omega}}(t) = \underline{\xi}(t) + \underline{v}(t), \quad (15)$$

where

$$\underline{\xi}(t) = \mathbf{I}^{-1}(\tilde{\omega}\mathbf{I}\underline{\omega}) \quad (16)$$

represents the nonlinear homogeneous function for the torque-free motion of a rigid body.

The following notation is used:  $t_i$  is the time of the  $i$ th control switch and

$$\Delta_i = t_i - t_{i-1}$$

$$\underline{\omega}_i = \underline{\omega}(t_i)$$

$$\underline{v}_i = \underline{v}(t_{i-1} \leq t \leq t_i)$$

$$\underline{\xi}_i = \int_{t_{i-1}}^{t_i} \underline{\xi}(t) dt.$$

Assuming that  $\underline{v}(t)$  is piecewise constant with bang-bang control, the angular velocity over the interval  $\Delta_i$  is given by

$$\underline{\omega}_i = \underline{\omega}_{i-1} + \underline{v}_i \Delta_i + \underline{\xi}_i. \quad (17)$$

Applying the boundary conditions  $\underline{\omega}_0 = \underline{\omega}_6 = \underline{0}$  gives

$$\sum_{i=1}^6 \underline{v}_i \Delta_i = - \sum_{i=1}^6 \underline{\xi}_i. \quad (18)$$

For a symmetric body,  $\underline{\xi}_i \equiv 0$ ,  $i = 1, \dots, 6$ , and it is shown by Byers and Vadali (1993) that

$$\Delta_{i+3} = \Delta_i \quad (19)$$

$$\underline{u}_{i+3} = -\underline{u}_i \quad i = 1, 2, 3, \quad (20)$$

where  $\underline{u}_i$  is the control vector over the time interval  $\Delta_i$ . In addition, for a rotation about a principal (i.e., control) axis, it is found that  $\Delta_1 = \Delta_3 = \Delta_4 = \Delta_6$ . For some special boundary conditions, one or more of the  $\Delta_i = 0$ , which indicates simultaneous switching of two or more controls.

For axisymmetric or nonsymmetric bodies, the switching pattern is somewhat more complicated. The effect of the gyroscopic precession terms in Euler's equations is to shift the switch times from the symmetry observed in equation (19). However, the five-switch pattern persists. Applying equation (20) in equation (18) and defining  $\delta_i = \Delta_i - \Delta_{i+3}$  gives

$$[\underline{v}_1 \quad \underline{v}_2 \quad \underline{v}_3] \underline{\delta} = - \int_0^{t_6} \underline{\xi}(t) dt. \quad (21)$$

The vector  $\underline{\delta}$  representing shifts or *skewing* of the symmetry of the switch times and is given by

$$\underline{\delta} = -\mathbf{V}^{-1} \int_0^{t_6} \underline{\xi}(t) dt, \quad (22)$$

where  $\mathbf{V}$  is the matrix of column vectors  $v_1$ ,  $v_2$ , and  $v_3$ . This may be written as

$$\underline{\delta} = \mathbf{U}^{-1} \mathbf{B}^{-1} \begin{Bmatrix} (I_2 - I_3) \int_0^{t_6} \omega_2 \omega_3 dt \\ (I_3 - I_1) \int_0^{t_6} \omega_1 \omega_3 dt \\ (I_1 - I_2) \int_0^{t_6} \omega_1 \omega_2 dt \end{Bmatrix}, \quad (23)$$

where  $\mathbf{U} = [u_1 \ u_2 \ u_3]$ . The switch-time skewing is an extremely nonlinear function of the boundary conditons and the moments of inertia. For a rotation of an axisymmetric body about the symmetry axis, it is observed that the skewing of the switch times by the gyroscopic precession is itself symmetric. That is,

$$\begin{aligned} \Delta_1 &= \Delta_6 \\ \Delta_2 &= \Delta_5 \\ \Delta_3 &= \Delta_4, \end{aligned} \quad (24)$$

giving

$$\begin{aligned} \delta_1 &= -\delta_3 \\ \delta_2 &= 0. \end{aligned} \quad (25)$$

Although it is not possible to directly compare the results for an axisymmetric body with those for a symmetric one, the contribution of the gyroscopic terms in Euler's equations can be observed. The solution for the actual motion may be compared to a solution of the same rotation in which the effect of the nonlinear terms in Euler's equations are neglected, that is,  $\underline{\omega} = \underline{v}$ . Consider a uniform oblate disk of unit mass with  $I_1 = I_2 = .51$ ,  $I_3 = 1 \Rightarrow \underline{\alpha} = [-.96 \ .96 \ 0]$  and  $\mathbf{B}$  is the  $3 \times 3$  identity matrix. This corresponds to a disk with a radius 4.08 time larger than its thickness and is close to the limiting condition for an infinitesimally thin disk with  $\underline{\alpha} = [-1 \ 1 \ 0]$ . In Figure 1, the angular velocity history is shown for the boundary conditions

$$\underline{\beta}(0) = [0.0 \ 0.0 \ 1/\sqrt{2} \ 1/\sqrt{2}]^T$$

$$\underline{\beta}(t_f) = [0.0 \ 0.0 \ 0.0 \ 1.0]^T.$$

The Euler axis,  $\underline{l}(0)$ , is parallel to the axis of symmetry and the Euler angle,  $\theta(0) = 90^\circ$ . It is important to note that the time optimal control is not unique for rotations about a principal axis. For both the actual and the notional motion, there are four trajectories with identical final times. The four trajectories correspond to all the possible combinations of initial signs of the two noncritical axes.

The maneuver depicted shows that there are five control switches, which coincide with the rate discontinuities in the angular velocity histories. The control associated with the critical axis switches once; the other two controls switch twice. The nonprecessing

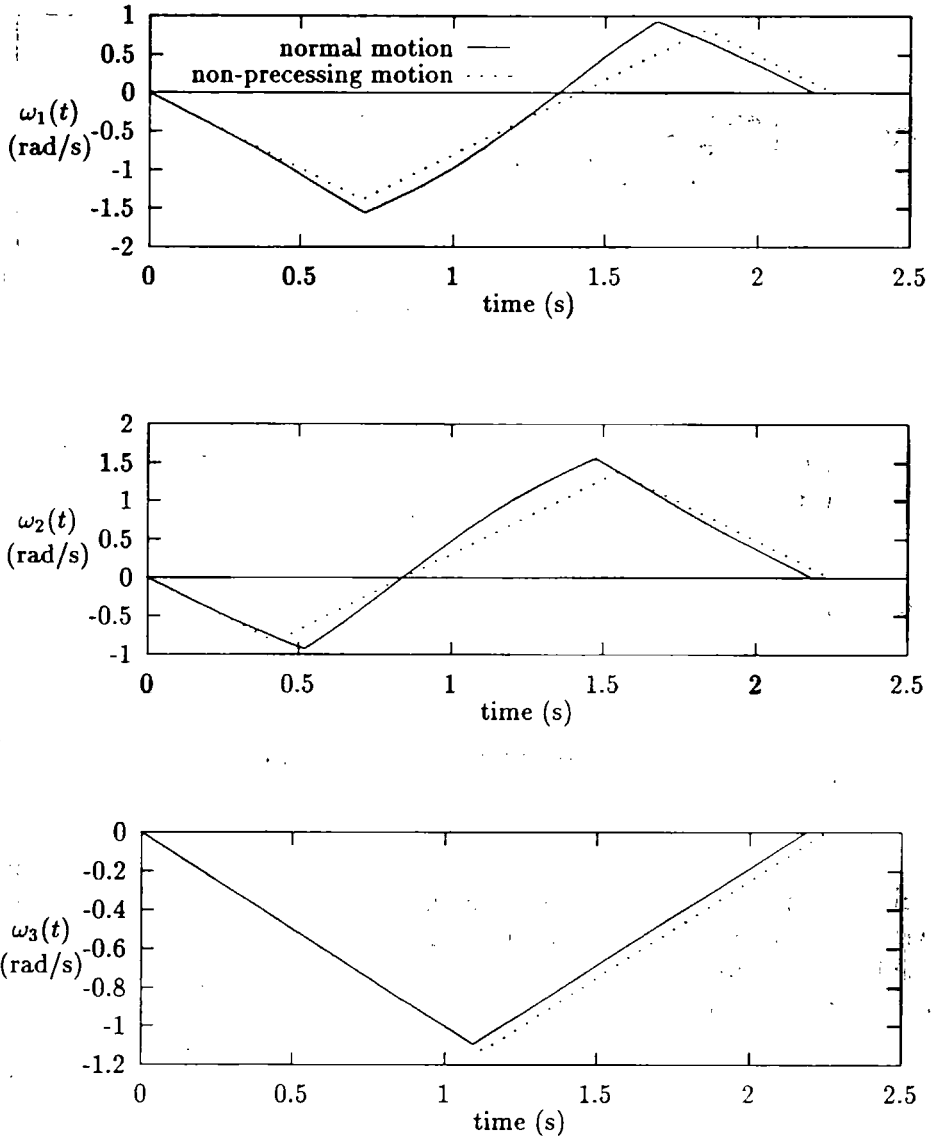


Figure 1. Symmetric body angular velocity history.

body exhibits the symmetry of equation (20), whereas the actual motion conforms to equation (24). As observed by Bilimoria and Wie (1993), the time optimal trajectory is not an eigenaxis type rotation. It is also observed that the net effect of the precession is to reduce the final time over that required for a fixed axis rotation. They found that the improvement in the final time over an eigenaxis rotation is greater for a disk than for a thin rod. For a prolate body, symmetric about the  $u_3$ -axis,  $I_1 > I_3$  and the sign of  $\alpha_1$  is the reverse of that of an oblate body. As  $\alpha_1 \rightarrow 1$ , the optimal final time and the nonprecessing final time approach the time required for an eigenaxis rotation. This case has been previously addressed in the discussion of singular controls.

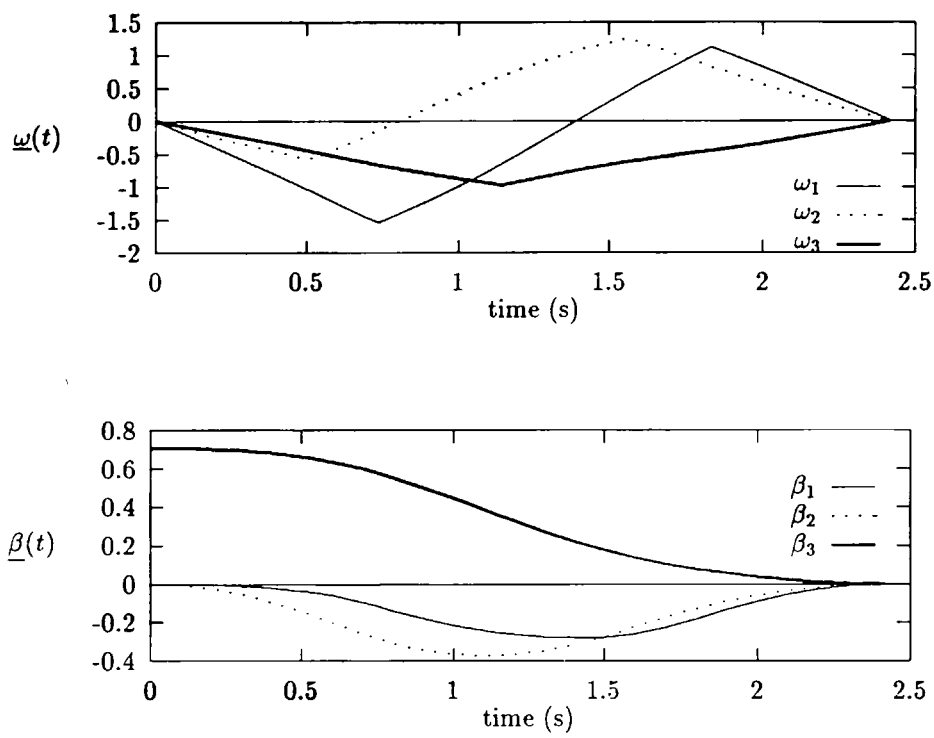


Figure 2. Time optimal rotation about  $u_3$  axis.

For a body with arbitrary moments of inertia, the skewing function is much too nonlinear and variable with boundary conditions to draw any general conclusions. The symmetry of the switch intervals of equation (19) no longer applies. Figure 2 shows a 90° rotation about the  $u_3$  axis of a body for which  $I_1 = .5$ ,  $I_2 = .8$ , and  $I_3 = 1.2 \Rightarrow \underline{\alpha} = [-.8 \ .875 \ -.25]^T$ . The control switch times occur at the rate discontinuities of the angular velocity plot. Again, although this is a minimum time solution, it is not unique. There are four switching sequences that yield the optimal final time. When the initial attitude of the body is also arbitrary, the switching is even more complex. The control symmetry of equation (20) appears no longer to apply unless some of the switch intervals are negative. Figure 3 illustrates this case. The body in the previous example is given the boundary conditions

$$\underline{x}(0) = [0.0 \ 0.0 \ 0.0 \ .231621 \ .3705929 \ .555889 \ .707106781]^T$$

$$\underline{x}(t_f) = [0.0 \ 0.0 \ 0.0 \ 0.0 \ 0.0 \ 0.0 \ 1.0]^T$$

The initial control vector is  $u_1 = [1.0 \ -1.0 \ -1.0]$  with the controls switching at the times shown in Table I.

In this particular maneuver, the  $u_3$  axis is the critical axis, as evidenced by the single switch of  $u_3$ . In the absence of precession, one would expect controls  $u_1$  and  $u_2$  each to switch once before and once after the switch of  $u_3$ . However, equation (20) still holds if it is permitted that  $\Delta_3 < 0$ .



Table I. Optimal switch times.

Control	Switch times (s)
$u_1$	0.41982
$u_3$	0.94538
$u_2$	1.04094
$u_1$	1.30375
$u_2$	1.94014
Cutoff	2.03297

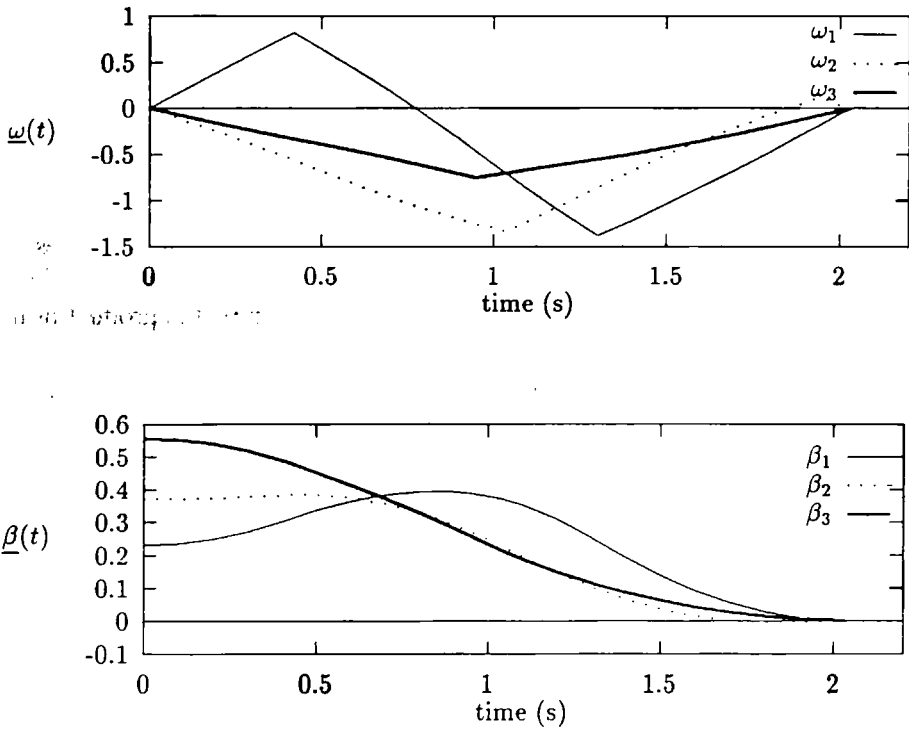


Figure 3. Time optimal rotation.

## 5. STATE TRANSITION MATRIX SOLUTION APPROACH

Equation (7) has the general solution

$$\underline{\beta}(t) = \Phi(t, t_0) \underline{\beta}(t_0), \quad (26)$$

where  $\Phi(t, t_0)$  is the state transition matrix, which satisfies the differential equations

$$\frac{d}{dt} \Phi(t, t_0) = \frac{1}{2} G(\underline{\omega}) \Phi(t, t_0) \quad (27)$$

with the initial conditions,  $\Phi(t_0, t_0) = E_4$ , the  $4 \times 4$  identity matrix.

Detailed analysis by Morton et al. (1974) of the state transition matrix reveals that there are only four unique elements giving  $\Phi(t, t_0)$  the antisymmetric structure

$$\Phi(t, t_0) = \begin{bmatrix} \phi_0 & -\phi_3 & \phi_2 & -\phi_1 \\ \phi_3 & \phi_0 & -\phi_1 & -\phi_2 \\ -\phi_2 & \phi_1 & \phi_0 & -\phi_3 \\ \phi_1 & \phi_2 & \phi_3 & \phi_0 \end{bmatrix}. \quad (28)$$

Thus the distinct elements of  $\Phi(t, t_0)$  are a vector of Euler parameters expressing instantaneous orientation relative to the final orientation. Defining the vector  $\underline{\phi}(t, t_0) = [\phi_1 \ \phi_2 \ \phi_3 \ \phi_0]^T$  and choosing  $\underline{\beta}(t_f) = [0 \ 0 \ 0 \ 1]^T$  results in

$$\underline{\phi}(t_f, t_0) = \underline{\beta}(t_0). \quad (29)$$

Assuming that the optimal maneuver is characterized by five switches of three controls, there are 48 possible control sequences. Twenty-four of these sequences may immediately be discarded as time optimal because they cause  $\ddot{\theta}_0(0) < 0$ , in which case the angle  $\theta$  would be increasing. If the critical axis is identified, and hence the control that switches only once, then there are only eight sequences that have potential for performing the maneuver. By applying the symmetry of equation (20) and allowing the switch intervals to have negative values, these eight sequences collapse to only four sequences. One of these sequences is the optimal control.

The state transition matrix for the entire maneuver is given by the product of the state transition matrices for each interval between switches.

$$\Phi(t_f, t_0) = \prod_{k=6}^1 \Phi(\Delta_k), \quad (30)$$

where  $\Phi(\Delta_i) = \Phi(t_i, t_{i-1})$ . The combination of equation (29) and the boundary conditions on angular velocity leads to the  $7 \times 1$  vector of nonlinear equations

$$\underline{f} = \left\{ \begin{array}{c} \underline{\phi}(t_f, t_0) - \underline{\beta}(t_0) \\ \underline{\omega}(t_f) \end{array} \right\} = \underline{0}, \quad (31)$$

where the elements of  $\underline{\phi}(t_f, t_0)$  are found via equation (30). The  $7 \times 6$  Jacobian matrix is defined

$$\mathbf{P} = \frac{\partial \underline{f}}{\partial \underline{\Delta}}, \quad (32)$$

where  $\underline{\Delta}$  is the vector of the six unique switch intervals.  $\mathbf{P}$  is found in this study via finite differencing. The switch interval vector  $\underline{\Delta}$  is found from an initial guess, using the pseudo-inverse and first-order Newton's method iteratively

$$\underline{\Delta}_{\text{new}} = \underline{\Delta}_{\text{old}} - \epsilon(\mathbf{P}^T \mathbf{P})^{-1} \mathbf{P}^T \underline{f}, \quad (33)$$

where  $\epsilon$  is a positive scalar less than one.

Thus the six unique control switch intervals may be determined by the above algorithm, provided that the elements of the state transition matrix for each interval are available.

## 6. TAYLOR SERIES SOLUTION OF THE STATE DIFFERENTIAL EQUATIONS

An analytical solution does not exist for equation (3) or equation (5); Morton et al. (1974) discuss a Taylor series expansion of these equations. This recursive solution to the Taylor series coefficients is presented below.

Define

$$\underline{\omega}_i^{(k)} = \left[ \frac{d^k \omega_i}{dt^k} \right]_{t=t_i} \quad i = 1, 2, 3. \quad (34)$$

For  $\underline{v}_i$  constant, successive differentiation of  $\underline{\omega}$  gives

$$\begin{aligned} \underline{\omega}_i^{(0)} &= \underline{\omega}_i \\ \underline{\omega}_i^{(1)} &= \mathbf{I}^{-1} \{ \tilde{\omega}_i^{(0)} \mathbf{I} \underline{\omega}_i^{(0)} \} + \underline{v} \\ \underline{\omega}_i^{(2)} &= \mathbf{I}^{-1} \{ \tilde{\omega}_i^{(1)} \mathbf{I} \underline{\omega}_i^{(0)} + \tilde{\omega}_i^{(0)} \mathbf{I} \underline{\omega}_i^{(1)} \} \\ \underline{\omega}_i^{(3)} &= \mathbf{I}^{-1} \{ \tilde{\omega}_i^{(2)} \mathbf{I} \underline{\omega}_i^{(0)} + 2\tilde{\omega}_i^{(1)} \mathbf{I} \underline{\omega}_i^{(1)} + \tilde{\omega}_i^{(0)} \mathbf{I} \underline{\omega}_i^{(2)} \} \\ &\vdots \end{aligned}$$

and yields the recursive formula

$$\underline{\omega}_i^{(k)} = \mathbf{I}^{-1} \{ c_{k,1} \tilde{\omega}_i^{(k-1)} \mathbf{I} \underline{\omega}_i^{(0)} + c_{k,2} \tilde{\omega}_i^{(k-2)} \mathbf{I} \underline{\omega}_i^{(1)} + c_{k,3} \tilde{\omega}_i^{(k-3)} \mathbf{I} \underline{\omega}_i^{(2)} + \dots + c_{k,k} \tilde{\omega}_i^{(0)} \mathbf{I} \underline{\omega}_i^{(k-1)} \}. \quad (35)$$

The binomial coefficients  $c_{k,i}$ ,  $i = 1, \dots, k$  are found recursively

$$\begin{aligned} c_{k,1} &= c_{k,k} = 1 \\ c_{k,i} &= c_{k,k-i} = c_{k-1,i-1} + c_{k-1,i} \quad i = 1, \dots, k/2 \\ c_{k,(k-1)/2+1} &= 2c_{k-1,(k-1)/2+1} \quad \text{for } k \text{ odd,} \end{aligned} \quad (36)$$

which gives Pascal's Triangle

	$i = 1$	2	3	4	5	6	$\dots$	$n$
$c_{1,i}$	1							
$c_{2,i}$	1	1						
$c_{3,i}$	1	2	1					
$c_{4,i} \Rightarrow$	1	3	3	1				
$c_{5,i}$	1	4	6	4	1			
$c_{6,i}$	1	5	10	10	5	1		
$\vdots$	$\vdots$							
$c_{n,i}$	1	$n-1$			$\dots$		$n-1$	1.

The angular velocity at the time of the  $i$ th control switch thus has the approximate solution

$$\underline{\omega}_i = \underline{\omega}_{i-1} + \sum_{k=1}^n \frac{\underline{\omega}_{i-1}^{(k)}}{k!} \Delta_i^k. \quad (37)$$

The state transition matrix, like the differential equations for angular velocity, may also be solved via a Taylor series. Adopting the notation

$$\Phi_i^{(k)} = \frac{d^k}{dt^k} \Phi(t, t_i) \Big|_{t=t_i} \quad (38)$$

the solution has the form

$$\Phi(t_i, t_{i-1}) = E_4 + \sum_{k=1}^n \frac{\Phi_{i-1}^{(k)}}{k!} \Delta_i^k. \quad (39)$$

Successive differentiation of equation (27) evaluated at the initial conditions gives

$$\begin{aligned} \Phi_i^{(0)} &= E_4 \quad 4 \times 4 \text{ identity matrix} \\ \Phi_i^{(1)} &= \frac{1}{2} G(\underline{\omega}_i^{(0)}) \Phi_i^{(0)} \\ \Phi_i^{(2)} &= \frac{1}{2} G(\underline{\omega}_i^{(1)}) \Phi_i^{(0)} + \frac{1}{2} G(\underline{\omega}_i^{(0)}) \Phi_i^{(1)} \\ \Phi_i^{(3)} &= \frac{1}{2} G(\underline{\omega}_i^{(2)}) \Phi_i^{(0)} + G(\underline{\omega}_i^{(1)}) \Phi_i^{(1)} + \frac{1}{2} G(\underline{\omega}_i^{(0)}) \Phi_i^{(2)} \\ \Phi_i^{(4)} &= \frac{1}{2} G(\underline{\omega}_i^{(3)}) \Phi_i^{(0)} + \frac{3}{2} G(\underline{\omega}_i^{(2)}) \Phi_i^{(1)} + \frac{3}{2} G(\underline{\omega}_i^{(1)}) \Phi_i^{(2)} + \frac{1}{2} G(\underline{\omega}_i^{(0)}) \Phi_i^{(3)} \\ &\vdots \\ \Phi_i^{(k)} &= \frac{1}{2} \{ c_{k,1} G(\underline{\omega}_i^{(k-1)}) + c_{k,2} G(\underline{\omega}_i^{(k-2)}) \Phi_i^{(1)} + c_{k,3} G(\underline{\omega}_i^{(k-3)}) \Phi_i^{(2)} + \dots + c_{k,k} G(\underline{\omega}_i^{(0)}) \Phi_i^{(k-1)} \}. \end{aligned} \quad (40)$$

Figure 4 illustrates a comparison of the exact solution of the elements of the state transition matrix found by direct integration of equation (27) with a 15-term truncated Taylor series solution for a body with  $I_1 = .5$ ,  $I_2 = .8$  and  $I_3 = 1.2$ . Because the maximum rotation to be considered is  $180^\circ$ , there is no need to consider a solution that is accurate over a greater range. In Figure 4, the body has rotated through  $180^\circ$  at  $\phi_0 = 0$ .

In the special case where there is no gyroscopic precession and the control and angular velocity vectors are parallel, the Taylor series has the exact solution

$$\begin{aligned} \phi_j &= -\frac{\gamma_j}{\|\underline{\gamma}\|} \sin\left(\frac{\|\underline{\gamma}\|}{2}\right) \quad j = 1, 2, 3 \\ \phi_0 &= \cos\left(\frac{\|\underline{\gamma}\|}{2}\right), \end{aligned} \quad (41)$$

where

$$\underline{\gamma} = \int_0^t \underline{\omega}(\tau) d\tau. \quad (42)$$

## 7. RAPID OPTIMAL SWITCH SOLUTION ALGORITHM

The Rapid Optimal Switch Solution (ROSS) algorithm has the following steps:

1. Identify the four possible initial control vectors that satisfy

$$\beta_1(0)v_1(0) + \beta_2(0)v_2(0) + \beta_3(0)v_3(0) > 0. \quad (43)$$

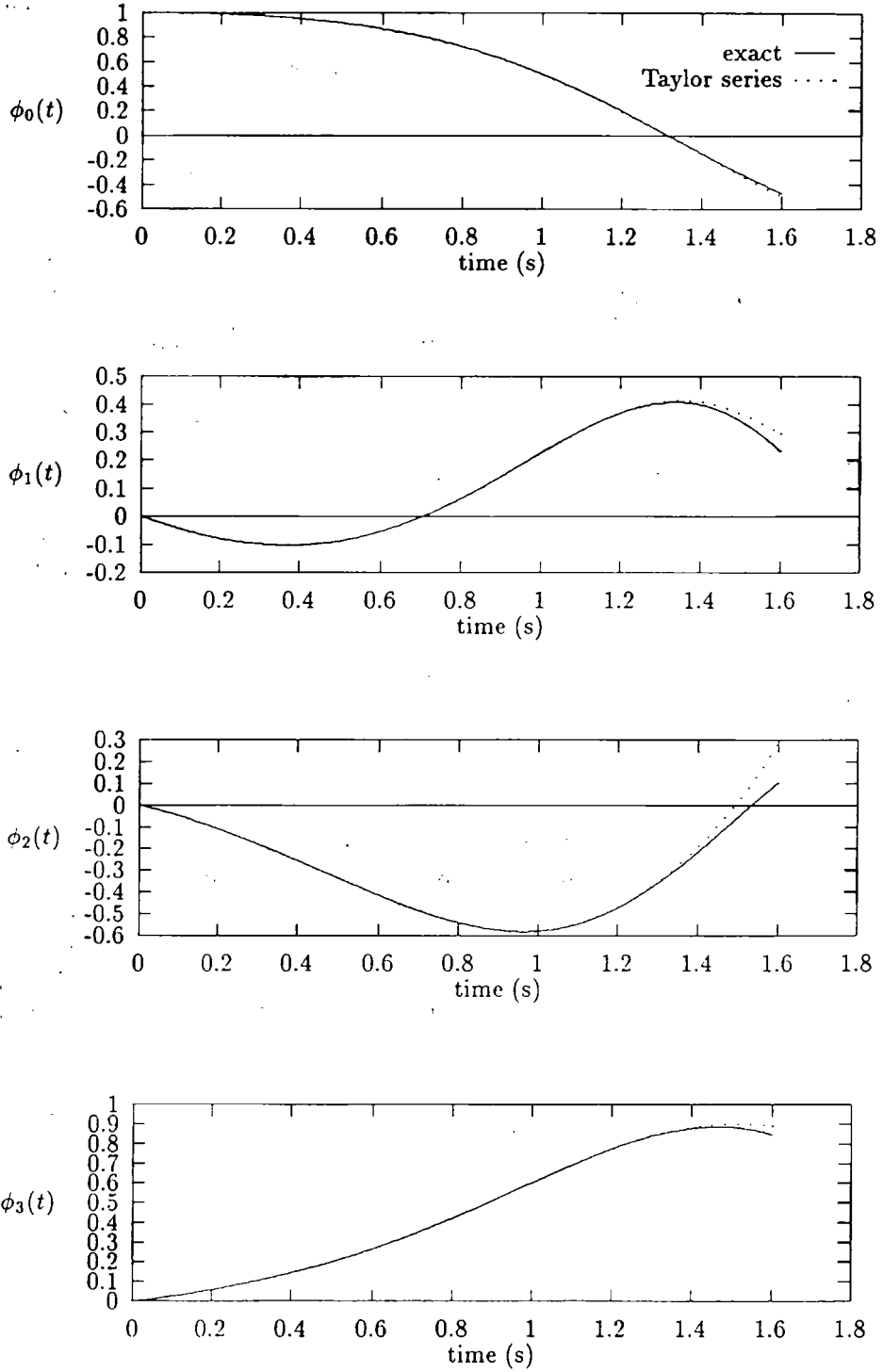


Figure 4. State transition matrix elements.

2. Determine the critical axis from the boundary conditions. The critical axis is identified as the largest component of  $\underline{\zeta} = \mathbf{B}^{-1}\mathbf{I}\underline{l}(0)$ .
3. Each of the four initial control vectors determined in 1 will have two possible sequences using the symmetry of equation (20) with the critical axis control switching once and the other two switching twice, giving a total of eight candidate switching sequences. Allowing time intervals to have negative values reduces this to four sequences, which must be tested.
4. Determine the initial guess of the switch times for a candidate sequence. The initial guess switch times have the symmetry of equation (19) and are found as in Byers and Vadali (1993) by solving

$$(\Delta_1 + \Delta_2 + \Delta_3)[\Delta_1 \quad \Delta_2 \quad \Delta_3]^T = -\theta(0)\mathbf{V}^{-1}\underline{l}(0). \quad (44)$$

5. Determine the value of  $\underline{f}$  in equation (31). The Jacobian  $\mathbf{P}$  is found using finite differencing of  $\underline{f}$ .
6. Iterate equation (33) until convergence.
7. Repeat steps 2 through 4 with the next sequence. The sequence solution with the shortest final time is the optimal solution. In the case where the initial Euler axis coincides with a principal axis, all four solutions will have the same final time.

## 8. RESULTS

The accuracy of the solution given by the above algorithm is dependent on the number of terms in the truncated Taylor series approximations of the angular velocity and the state transition matrix elements. The number of terms used affects the time needed for solution as does the convergence tolerance demanded. By trial it has been determined that approximately 15 terms are required for each series to be essentially exact for continuous rotations of  $180^\circ$ . In the case of rest-to-rest rotations, the maximum rotation angle is  $180^\circ$ . However, the maximum rotation between control switches cannot be greater than  $90^\circ$ . In fact, for most maneuvers, the angle traversed between switches is far less. In the solutions shown below, the angular velocity and Euler parameter approximations each contain 10 terms. This number gives essentially exact results for symmetric and axisymmetric bodies. Increasing the number of Taylor series terms to 15 gives essentially exact results for arbitrary bodies.

Two example maneuvers are shown with the same parameters as those for the maneuvers in Figures 2 and 3. The first maneuver is a  $90^\circ$  rotation with the Euler axis initially coincident with the body fixed  $u_3$  axis. The initial conditions

$$\underline{x}(0) = [0.0 \quad 0.0 \quad 0.0 \quad 0.0 \quad 0.0 \quad .707106781 \quad .707106781]^T$$

$$\underline{x}(t_f) = [0.0 \quad 0.0 \quad 0.0 \quad 0.0 \quad 0.0 \quad 0.0 \quad 1.0]^T$$

are the same as those for the maneuver in Figure 2. The initial control is given by

$$\underline{u}(0) = \begin{Bmatrix} -1.0 \\ -1.0 \\ -1.0 \end{Bmatrix}.$$

Table II. Optimal and estimated switch times.

<i>Control</i>	<i>STO (s)</i>	<i>ROSS (s)</i>
$u_2$	0.50913	.50736
$u_1$	0.73666	.73691
$u_3$	1.13876	1.14679
$u_2$	1.56300	1.56339
$u_1$	1.83402	1.83345
Cutoff	2.41956	2.41964

Table III. Optimal and estimated switch times.

<i>Control</i>	<i>STO (s)</i>	<i>ROSS (s)</i>
$u_1$	0.41982	0.42001
$u_3$	0.94538	0.94557
$u_2$	1.04094	1.04104
$u_1$	1.30375	1.30417
$u_2$	1.94014	1.94056
Cutoff	2.03297	2.03330

As discussed before, the solution is not unique in this type of maneuver. Table II shows the switching sequence and switch times found by solution by the TPBVP by the STO algorithm and compares them to the times predicted by the ROSS algorithm. Iteration is halted when  $|\Delta_{i_{\text{new}}} - \Delta_{i_{\text{old}}}| \leq .00001$ ,  $i = 1, \dots, 6$ . In principal axis maneuvers, it is possible to exploit the fact that all sequences give the same final time. This solution of this example required 3.2 seconds of CPU time on a Sun Sparc 1+ workstation.

The second example has the same initial conditions as those for the maneuver in Figure 3

$$\underline{x}(0) = [0.0 \quad 0.0 \quad 0.0 \quad .231621 \quad .3705929 \quad .555889 \quad .707106781]^T$$

$$\underline{x}(t_f) = [0.0 \quad 0.0 \quad 0.0 \quad 0.0 \quad 0.0 \quad 0.0 \quad 1.0]^T.$$

The initial control vector is  $u_1 = [1.0 \quad -1.0 \quad -1.0]$  with the controls switching as shown in Table III. Solving all four candidate switching sequences required 12.1 seconds on a Sun SPARC 1+ workstation. This second maneuver demonstrates the ability of the ROSS algorithm to accommodate switching sequences, which do not possess the symmetry assumed in equation (20) by allowing negative switch interval times.

## 9. CONCLUSIONS

The time optimal reorientation of a rigid body has been examined for an asymmetric rigid body. It has been shown that there is no possibility for singular arcs for physically realizable bodies and that the large angle rotation can be characterized by five control switches. The consistent behavior of the switching pattern has led to a method for rapidly solving the time optimal switch times. The speed with which the ROSS algorithm obtains solutions to the switch times is in sharp contrast to that required for other numerical solutions. The STO algorithm, for example, requires an initial guess of the initial control vector, the switch times, and the final time. Depending on the error tolerance for convergence, it may take several minutes of computation to solve, even with a good initial guess. The ROSS algorithm, in contrast, requires no initial guess and converges within seconds with only modest computational power. For symmetric bodies, computation time is further reduced, because only two Taylor series terms are required for an exact solution to the angular velocity. The solution time is a function of the number of terms in the Taylor series approximation, and is fairly insensitive to the size of the rotation. This feature makes it attractive for possible on-line implementation.

## REFERENCES

- Bilimoria, K. D. and Wie, B., 1991, "Time-optimal reorientation of a rigid axisymmetric spacecraft," *AIAA Paper 91-2644, Guidance, Navigation and Control Conference*, Portland, OR, August, 1991.
- Bilimoria, K. D. and Wie, B., 1993, "Minimum time large angle reorientation of a rigid spacecraft," *Journal of Guidance, Control, and Dynamics* **16**(3), 446-452.
- Byers, R. M., 1995, "On singular controls in time optimal rigid body reorientation," *AAS 95-138, AAS/AIAA Spaceflight Mechanics Conference*, Albuquerque, NM, February, 1995.
- Byers, R. M. and Vadali, S. R., 1993, "Quasi-closed form solution to the time-optimal rigid spacecraft reorientation problem," *Journal of Guidance, Control, and Dynamics* **16**(3), 453-461.
- Meier, E. B. and Bryson, A. E., 1990, "Efficient algorithm for time optimal control of a two-link manipulator," *Journal of Guidance, Control, and Dynamics* **13**(5), 859-866.
- Morton, H. S., Junkins, J. L., and Blanton, J. N., 1974, "Analytical solutions for Euler parameters," *Celestial Mechanics* **10**, 287-301.
- Seywald, H. and Kumar, R., 1993, "Singular control in minimum time spacecraft reorientation," *Journal of Guidance, Control, and Dynamics* **16**(4), 686-694.
- Tsiotras, P. and Longuski, J. M., 1991, "A complex analytic solution for the attitude motion of a near-symmetric rigid body under body-fixed torques," *Celestial Mechanics and Dynamical Astronomy* **51**, 281-301.